J Mater Sci (2010) 45:6719–6726
DOI 10.1007/s10853-010-4765-0

# Microstructural characterization of M250 grade maraging steel using nonlinear ultrasonic technique

**A. Viswanath · B. P. C. Rao · S. Mahadevan · T. Jayakumar · Baldev Raj**

Received: 11 March 2010 / Accepted: 10 July 2010 / Published online: 23 July 2010


**Abstract** Nonlinear ultrasonic (NLU) technique is used for characterization of microstructures in M250 grade maraging steel subjected to solution annealing at 1093 K for 1 h followed by ageing at 755 K for various ageing durations in the range from 0.25 to 100 h. Using pulse inversion technique, feeble second harmonic is extracted to determine nonlinear ultrasonic parameter, $\beta$, and the relative $\beta$ parameter (RBP) which is the ratio of $\beta$ parameter of the precipitation hardened specimen to that of the solution annealed specimen. Normalized mean square strain, volume fraction of reverted austenite and hardness have been measured and transmission electron microscopy (TEM) has been carried out to understand the microstructural changes that occur during ageing and to study the correlation between these measured parameters. Hardness and normalized mean square strain are found to increase during initial stages of ageing due to precipitation of intermetallics and decrease at longer durations due to formation of reverted austenite and coarsening of precipitates. This study establishes that NLU technique can be used for non-destructive characterization of ageing behaviour of M250 grade maraging steel.

## Introduction

Maraging steels are low-carbon ultra high-strength precipitation hardenable martensitic steels. They possess excellent mechanical properties such as good fracture toughness, high strength to weight ratio, good weldability, resistance to hydrogen embrittlement and stress corrosion cracking [1]. These superior properties make the maraging steel to be used widely in several demanding applications including aerospace rocket motor casings, aircraft forgings, tools and dies and rotor parts of ultracentrifuges.

The precipitation behaviour and microstructural aspects of various grades of maraging steels have been extensively studied [2–11]. Maraging steels consist of martensitic structure with high dislocation density in the solution annealed condition and harden due to the precipitation of intermetallic precipitates. During the initial stages of ageing, recovery of martensitic structure and hardening due to precipitation of hexagonal $Ni_3Ti$ intermetallic precipitates takes place [2, 4]. It is observed that the recovery of martensitic structure is characterized by annihilation of dislocations and internal dislocation substructural changes that reduce the dislocation density [2, 12]. During the intermediate stages of ageing, precipitation of hexagonal $Fe_2Mo$ intermetallic precipitates occurs. It is also observed that size and volume fraction of $Ni_3Ti$ and $Fe_2Mo$ precipitates increase with ageing time and the precipitates become semi-coherent after growing beyond a critical size of approximately 10 nm (>10 h ageing) [6]. At longer ageing duration, formation of reverted austenite takes place and the volume fraction of reverted austenite increases with ageing duration [6]. It is reported that the best combination of mechanical properties in M250 grade maraging steel components, i.e. ultra-high strength and good fracture toughness, is obtained by solution annealing (SA) treatment at 1093 K for 1 h followed by ageing at 755 K for 3–10 h through the precipitation of intermetallic phases in low-carbon soft martensitic matrix [6]. Coarsening of the intermetallic precipitates and formation of reverted

A. Viswanath · B. P. C. Rao (✉) · S. Mahadevan · T. Jayakumar · Baldev Raj
Non-Destructive Evaluation Division, Metallurgy and Materials Group, Indira Gandhi Centre for Atomic Research, Kalpakkam 603102, Tamil Nadu, India
e-mail: bpcrao@igcar.gov.in

austenite are detrimental to the tensile and fracture properties. The over-aged intermetallic precipitates serve as crack nucleation sites and hence, increase the brittleness [13]. The reverted austenite is a soft phase. Under loading conditions, the deformation is concentrated in the reverted austenite regions, which reach their critical strain to fracture at an early stage, thus degrading the mechanical properties. Hence, non-destructive detection of coarsening of the precipitates and formation of reverted austenite in maraging steel is desired.

Several researchers used ultrasonic [12], eddy current [14, 15], magnetic Barkhausen emission [16, 17], X-ray diffraction (XRD) [18, 19] and positron annihilation [20] techniques for nondestructive characterization of microstructures in M250 grade maraging steel. Hardness and ultrasonic velocities (shear as well as longitudinal) are reported to exhibit similar behaviour upon ageing, i.e. they increase with volume fraction of intermetallic precipitates and decrease with austenite reversion. It is also observed that the Poisson's ratio, determined from the ultrasonic longitudinal and shear wave velocities, decreases monotonously with ageing time [12]. Pardal et al. [16] have studied the influence of ageing temperature and time on magnetic properties of 300 grade maraging steel and reported that a good correlation (square function) between saturation magnetization and amount of austenite exists and this can be used to estimate the austenite volume fraction in maraging steels. XRD technique has been employed to study the microstrains developed during precipitation of intermetallic phases [18]. It is reported that the microstrains increase up to 10 h of ageing due to precipitation of fine and coherent intermetallic precipitates and then decrease beyond 10 h due to loss of coherency strains as a result of coarsening of the precipitates and formation of the reverted austenite [18].

Nonlinear ultrasonic (NLU) technique, wherein high amplitude ultrasonic waves of a particular frequency are made to propagate through the material and the harmonics generated due to nonlinear (elastic and plastic) interaction of ultrasonic waves with lattice defects or substructural changes are detected and used for material characterization and assessment of damage in structural materials. NLU technique is useful for studying the influence of dislocation density, dislocation arrangement, precipitates and microcracks [21–37]. This technique can overcome the limitations of the conventional linear ultrasonic technique for studying the nonlinear behaviour of materials, as reported by Hurley et al. [23] and Jhang [32].

The nonlinear parameter, $\beta$, is a strong function of dislocation density [21–23], precipitate coherency strains [24–28], fatigue promoted dislocation dipoles [29–32] and the residual stress in the material [34]. Hikata et al. [21] carried out theoretical and experimental studies in aluminium single crystals subjected to bias stress and established a linear dependence of $\beta$ parameter with dislocation density. Similarly, Hurley et al. [23] used NLU technique for microstructural characterization of quenched martensitic steels with varying carbon content and reported that $\beta$ parameter increases with increase in dislocation density. Cantrell et al. [24–26] studied the kinetics of precipitation and effects of coherency strains in the aluminium alloy (Al 2024) using NLU technique and observed that precipitate matrix coherency strains will significantly influence the nonlinear behaviour of the material. They also reported that $\beta$ parameter is a function of precipitate–matrix misfit parameter and volume fraction of the precipitates. NLU technique has also been used for early fatigue damage assessment in aluminium 2024-T4 [29], Ti-6Al-4V [30], SS41 grade mild steel and SS45 grade mild steel [31, 32]. In these materials, fatigue damage progresses by increase in dislocation density, dislocation substructural changes and formation of micro-cracks and voids before its failure. In general, it is observed that the $\beta$ parameter increases significantly with increase in number of fatigue cycles the material has undergone and it reaches saturation before the material fails, i.e. approximately after 60–70% of fatigue life [29, 30], which is attributed to the increase in dislocation density and the dislocation dipole substructural development. Recently, Pruell et al. [33] have reported the existence of a fundamental relationship between the material plasticity and the ultrasonic nonlinearity behaviour of the material, independent of the interacting wave type, i.e. longitudinal, Rayleigh and lamb waves. They reported that the residual stress in the material arising due to statically induced plastic strain will increase the ultrasonic nonlinearity parameter.

During ageing of M250 grade maraging steel, reduction in dislocation density, precipitation of $Ni_3Ti$ and $Fe_2Mo$ precipitates and reversion of austenite take place at varying durations and these changes would strongly influence the nonlinear behaviour of this material. Metya et al. [34] studied the ageing behaviour of similar steel, i.e. C-250 grade maraging steel and reported that nonlinear parameter increases till the precipitates are semi-coherent and finer and decreases at longer ageing durations due to coarsening of precipitates. However, they have not quantitatively analyzed the effect of change in coherency strains and volume fraction of reverted austenite which is reported to influence various NDE parameters [12, 14–17]. In the present study, NLU technique has been used for characterization of microstructures in precipitation hardened M250 grade maraging steel specimens aged at 755 K for various durations in the range from 0.25 to 100 h. This study also aims at quantitatively studying the influence of coherency strains and reverted austenite on the NLU parameter. This paper explains the theory of nonlinear

ultrasonic technique and the experimental procedure followed to measure the fundamental and second harmonic amplitudes used to determine the nonlinear ultrasonic parameter, $\beta$. The paper discusses the changes in $\beta$ with ageing time based on normalized mean square strain, volume fraction of reverted austenite using XRD and microstructural changes by TEM.

## Theory of nonlinear ultrasonic technique

The linear stress–strain relationship given by Hooke's law is valid for a homogenous and isotropic medium when the applied stress amplitude is infinitesimal. However, materials in nature exhibit nonlinear stress–strain relationship and this can be represented by power series expansion of strain as given by Eq. 1,

$$\sigma = A\varepsilon + \frac{1}{2}B\varepsilon^2 + \cdots \tag{1}$$

where $\sigma$ is stress, $\varepsilon$ is displacement gradient, $A$ is the coefficient of second order term and $B$ is the coefficient of third order term which is a combination of second and third order elastic constants [30, 35]. The equations of motion of a solid element in the absence of body forces is given by Eq. 2,

$$\rho\frac{\partial^2 u}{\partial t^2} = \frac{\partial \sigma}{\partial x} \tag{2}$$

where $\rho$ is the density of material, $x$ is the propagation distance of sound wave, $u$ is the displacement in the $x$ direction. Using the relationship between strain and displacement, i.e. $\varepsilon(x,t) = \partial u(x,t)/\partial x$ and considering the propagation of one dimensional longitudinal wave ($u = A_1 \sin \omega t$, $A_1$ is amplitude, $k$ is wave number and $\omega$ is angular frequency) through the isotropic material and substituting Eq. 1 in Eq. 2 one gets

$$\rho\frac{\partial^2 u}{\partial t^2} = A\frac{\partial^2 u}{\partial x^2} + B\frac{\partial u}{\partial x}\frac{\partial^2 u}{\partial x^2} \tag{3}$$

A perturbation solution is assumed to solve Eq. 3 and the solution after two iterations is given by [30, 35, 36]

$$u(x,t) = A_1 \sin(kx - \omega t) - \frac{1}{8}\frac{B}{A}k^2 A_1^2 x \cos[2(kx - \omega t)] + \cdots \tag{4}$$

From Eq. 4, the expression for the second harmonic amplitude, $A_2$, is expressed as

$$A_2 = \frac{1}{8}\left(\frac{B}{A}\right)A_1^2 k^2 x \tag{5}$$

In Eq. 5, $B/A$ term represents the nonlinear parameter $\beta$ and upon rearranging this can be expressed as

$$\beta = \frac{8}{k^2 x}\left(\frac{A_2}{A_1^2}\right) \tag{6}$$

Hence, the $\beta$ parameter of a material can be evaluated by measuring the amplitudes of the fundamental and second harmonic components and can be correlated to the changes responsible for the nonlinear behaviour of the material.

## Experimental

### Specimens

The chemical composition (wt%) of the M250 grade maraging steel used in this study is as follows: 17.89 Ni, 8.16 Co, 4.88 Mo, 0.43 Ti, 0.05 Mn, 0.05 Cr, 0.05 Si, 0.05 Cu, 0.096 Al, 0.003 C, balance Fe. A plate of M250 grade maraging steel is solution annealed (SA) at 1093 K for 1 h followed by air cooling. Specimens of dimensions 30 × 25 × 7 mm$^3$ cut from the SA plates were encapsulated in quartz tubes under vacuum and aged at 755 K for different durations of 0.25, 1, 3, 10, 30, 40, 70 and 100 h followed by water quenching.

Subsequently, the specimens were polished with 400 grit SiC emery paper to obtain uniform surface finish and plane parallelness for nonlinear ultrasonic measurements. Hardness, transmission electron microscopy (TEM) and selected area diffraction (SAD) analysis were carried out as detailed elsewhere [12]. Vickers hardness measurements were made at 10 kg load and the maximum scatter in the hardness measurements was found to be ±5 HV10. TEM studies were carried out on thin foil specimen using Philips M200 operated at 200 keV. Further, XRD measurements were carried out on precipitation hardened specimens using a MAC Science MXP18 X-ray diffractometer with Cu-K$\alpha$ radiation. The XRD spectra were recorded in the angular range from 36° to 122° with a step size of 0.02° and a dwell time of 4 s. The XRD peak profile corresponding to each plane was extracted for all the specimens by fitting a linear background along with a pseudo-Voigt function after accounting for instrumental broadening as detailed by Mahadevan et al. [18]. The full width at half maximum (FWHM), integral breadth and peak location were estimated from the individual XRD peak profiles for aged specimens and modified Williamson-Hall plots were made to determine the slope, i.e. the normalized mean square strain, $\alpha$ in the matrix [18].

### Nonlinear harmonic measurement setup

The schematic of the experimental setup used for NLU studies is shown in Fig. 1. It consists of a high power sinusoidal ultrasonic tone burst wave generator, pre-amplifier,

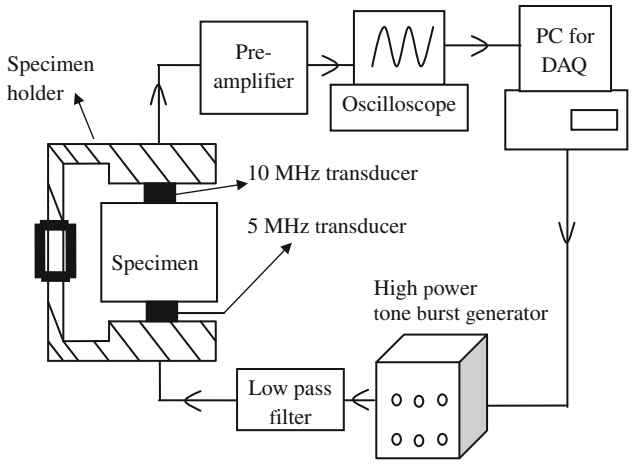


**Fig. 1** Experimental setup used for nonlinear ultrasonic measurements

high and low pass filters, digital storage oscilloscope and a personal computer for control and data acquisition. The power level of the tone burst generator is variable. A 5 MHz resonant piezoelectric ultrasonic transducer is used as transmitter and a 10 MHz broad band piezoelectric ultrasonic transducer is used as receiver. The number of cycles in the tone burst is optimized at eight cycles based on the sample thickness (7 mm) and ultrasonic velocity (5550 m/s). A pulse repetition frequency of 80 Hz is chosen for non-overlapping of pulse trains. The ultrasonic transducers are firmly fixed to the specimen using a specimen holder as shown in Fig. 1, to avoid pressure variations during the NLU measurements. The receiver output is fed to the digital storage oscilloscope and the time domain waveform data is stored for analysis. As the second harmonic amplitudes are very weak (approximately 1% of fundamental), pulse inversion technique [36–38] is used in this study to extract the second harmonic component. In pulse inversion technique, transmitted wave is superposed with another transmitted wave that is phase shifted by 180°. This superposition will result in cancellation of odd harmonics and in turn, amplification of the second harmonic amplitude.

The fundamental and second harmonic amplitudes for each precipitation hardened specimen are measured at different power levels in the range of 40% (300 V) to 80% (700 V). A plot is made between $A_2$ and $A_1^2$ for different power levels for each specimen and the slope of the plot is determined to obtain $\beta$, following Eq. 6. In the present work, the measured $A_1$ and $A_2$ are the amplitudes of the fundamental and second harmonic components in the uncalibrated electrical signals which are proportional to the absolute particle displacements $A_1$ and $A_2$, respectively, defined in Eq. 6 as discussed elsewhere [36]. In this study, as we are interested in studying the relative change in the nonlinear behaviour of the precipitation hardened specimens with respect to solution annealed condition, we have used relative $\beta$ parameter (RBP), which is the ratio of the $\beta$ parameter of the precipitation hardened specimen to that of the solution annealed specimen ($\beta_{Sample}/\beta_{SA}$). The RBP has been determined for SA and all the specimens aged in the range from 0.25 to 100 h.

## Results and discussion

Figure 2 shows the time-domain wave form of tone burst ultrasonic signal with an incident phase angle 0° and 180° (phase shifted) along with the resultant superposed signal, acquired from solution annealed specimen. Figure 3 shows the absolute amplitude of Fourier transform of the 0° tone burst and the superposed signal. As the absolute amplitude of Fourier transform of 0° tone burst and 180° phase-shifted tone burst are similar, the later has not been plotted. From Fig. 3, it is observed that fundamental frequency component is completely eliminated in the superposed signal leaving only the amplified second harmonic component. Hence, it is possible to measure the feeble second harmonic component by adopting the pulse inversion technique. In order to determine the $\beta$ parameter, $A_1$ is measured from the absolute amplitude of Fourier transform of 0° tone burst and $A_2$ is measured from the absolute amplitude of Fourier transform of superposed signal. Figure 4 shows the typical plot between $A_2$ and $A_1^2$ as a function of increasing power level (300–700 V) for solution annealed specimen. There exists a linear correlation between $A_2$ and $A_1^2$ with a correlation coefficient of 99.8%. Similar plots are made for all the age hardened specimens to determine nonlinear $\beta$ parameter and thereby RBP.

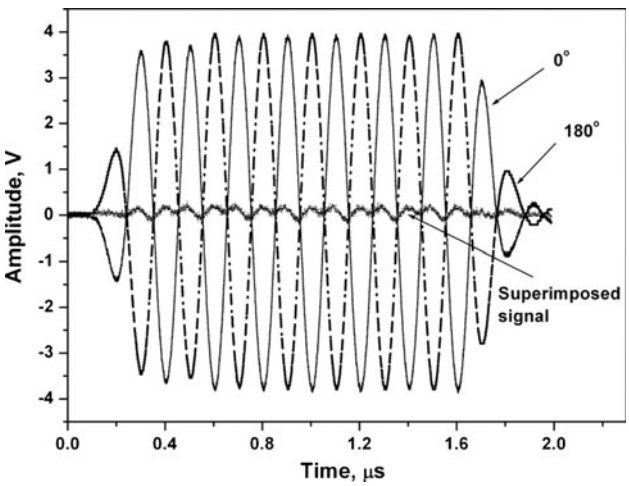


**Fig. 2** The tone burst ultrasonic signal with an incidental phase angle of 0° and 180° (phase-shift) and the superimposed signal for the solution annealed specimen

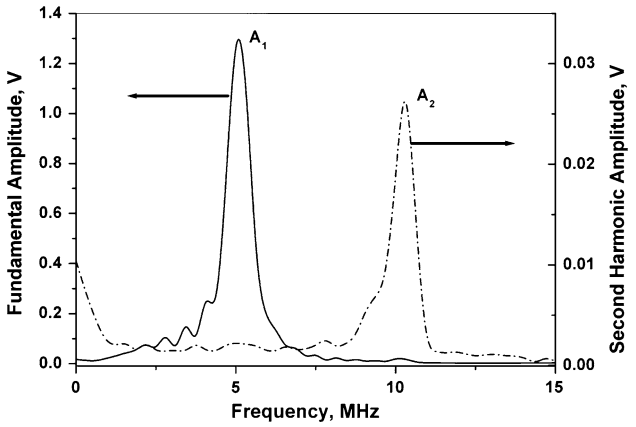


**Fig. 3** Absolute amplitude of Fourier transform of the 0° tone burst and the superposed signal, i.e. second harmonic obtained by pulse inversion technique

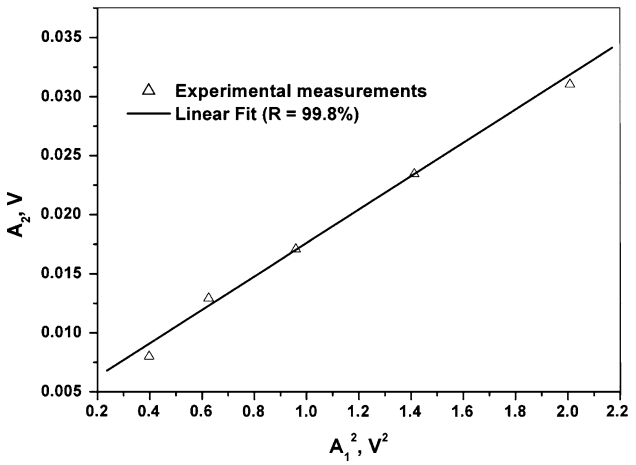


**Fig. 4** Variation of $A_2$ and $A_1^2$ with increase in power level for the solution annealed specimen

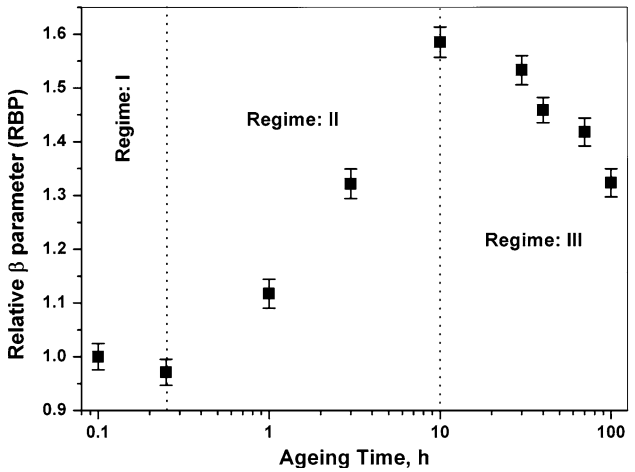


**Fig. 5** Variation of relative $\beta$ parameter with ageing time at 755 K

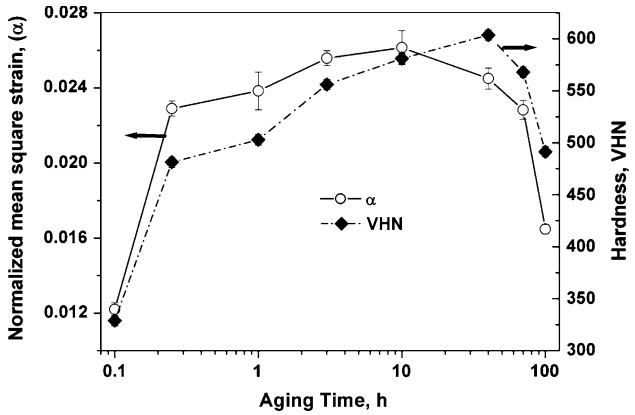


**Fig. 6** Variation of normalized mean square strain, α, and hardness with ageing time at 755 K

Figure 5 shows the variation of RBP as a function of ageing time for M250 grade maraging steel. Figure 6 shows the variation of normalized mean square strain (α) and hardness (VHN) with ageing time. From Fig. 5, it is observed that RBP changes systematically with ageing duration and these changes are analyzed by dividing in three regimes as shown in Fig. 5. The first regime (SA–0.25 h) is characterized by a marginal decrease in RBP up to 0.25 h of ageing and the second regime (0.25–10 h) is characterized by drastic increase in RBP and followed by a third regime (10–100 h) where RBP is found to decrease with ageing time.

During the initial stages of ageing up to 0.25 h, i.e. first regime, RBP is slightly decreased by 2.9%. This initial decrease in RBP is attributed to the combined effect of two counter acting mechanisms operating simultaneously during the initial stages of ageing. The first mechanism is the recovery of martensitic structure, i.e. annihilation of dislocations and rearrangement of dislocation internal substructure which results in the decrease of dislocation density. The bright field image of SA is shown in Fig. 7a. It is observed that this specimen is characterized by the presence of lath martensite with high dislocation density. It is well established that during initial stages of ageing treatment the recovery of martensitic structure is one of the major mechanism that takes place in this material [2, 6, 12]. The recovery of martensitic structure is characterized by dislocation annihilation and dislocation substructural changes. Annihilation of dislocations during initial stages of ageing of similar steel has been reported by Mahadevan et al. [18]. It is reported that the increase in crystallite size from 370 to 1248 Å from SA to 0.25 h is attributed to annihilation of dislocations during initial stages of ageing. It is also reported that ageing above 0.25 h does not change the crystallite size significantly, i.e. most of the dislocation annihilation activity is predominant in the first regime and thereafter dislocation density remains almost constant with ageing time. Hence, this decrease in dislocation density is

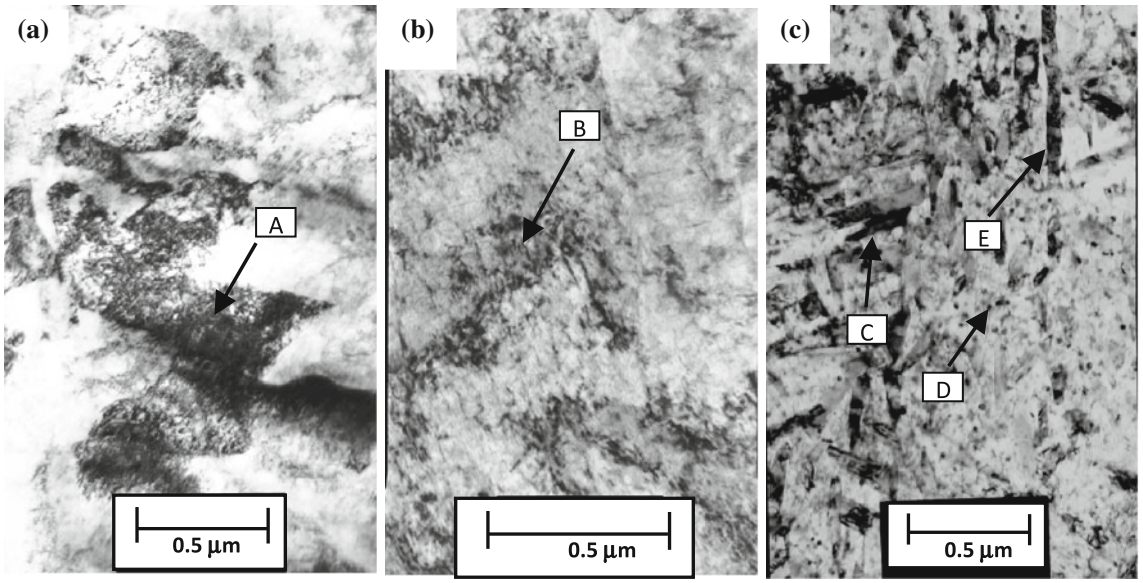


**Fig. 7** Bright field images of **a** solution annealed specimen showing high dislocation density in lath martensite (marked as *A*) and specimens aged at 755 K for **b** 3 h showing relatively low dislocation density in the martensite laths (marked as *B*) and **c** 100 h showing coarsened patchy $Ni_3$(Ti, Mo) (marked as *C*), globular $Fe_2Mo$ (marked as *D*) and long and patchy austenite (marked as *E*)

expected to decrease nonlinearity parameter, RBP, of this material and is given by Eq. 7,

$$\beta \propto NL^4\sigma \tag{7}$$

where $N$ is the dislocation density, $L$ is the dislocation loop length and $\sigma$ is the applied bias stress [21].

The second mechanism is increase in microstrain due to precipitation of very fine and coherent $Ni_3Ti$ intermetallic precipitates at dislocations and interlath boundaries as shown in Fig. 6. Vasudevan et al. [2] and Mahadevan et al. [18] have also reported that the microstrain and hardness increase during initial stages of ageing due to precipitation of fine $Ni_3Ti$ intermetallic precipitates which are coherent with the martensitic matrix. Hence, this increase in microstrain causes increase in RBP which has also been reported by Cantrell et al. [26] in Al 2024 alloy. Thus, a combined effect of these two counteracting mechanisms (i) decrease in dislocation density which should have decreased RBP and (ii) increase in microstrain which should have increased RBP is felt during the initial stages of ageing up to 0.25 h and causing a net marginal decrease of RBP by 2.9% which is measured precisely using pulse inversion technique.

During the intermediate stages of ageing, i.e. second regime (0.25–10 h) RBP is found to increase as a function of ageing time and reaches a peak value at 10 h with the formation of fine and coherent $Fe_2Mo$. The increase of RBP in 10 h aged specimen with respect to the solution annealed specimen is found to be approximately 60%. The TEM examination (BF image) of 3 h aged sample revealed the formation of very fine needle/rod-shaped precipitates as shown in Fig. 7b. For elucidation of increase in RBP and microstrain during the second regime, we have plotted variation of RBP and normalized mean square strain with respect to hardness as shown in Fig. 8. It is evident from Fig. 8 that, during the second ageing regime, RBP and $\alpha$ continue to increase with increase in hardness. In general, it is well known that the lattice parameter of the matrix material and the precipitate are different and this lattice mismatch will result in initiation of microstrain at the precipitate–matrix interface. Hence, the formation and growth of fine and coherent $Ni_3Ti$ and $Fe_2Mo$ intermetallic precipitates during this regime has resulted in increase in microstrain as shown in Fig. 8 and thus, the RBP, as given by Eq. 8,

$$\frac{\beta}{\beta_0} = -\left(3+\frac{12}{\beta_0}\right)\delta f_p^{1/3}\left(2.25-0.25f_p^{2/3}\right) \tag{8}$$

where $\beta_o$ is nonlinear ultrasonic parameter in the solution annealed condition, $\delta$ is precipitate–matrix misfit parameter and $f_p$ is the volume fraction of precipitate [25]. In the maraging steel, the lattice mismatch between martensitic matrix and precipitates is in the order of 2.22% and 4.9% for $Ni_3Ti$ and $Fe_2Mo$ intermetallic precipitates, respectively [39]. Mahadevan et al. [18] reported that volume fraction of precipitates increases with ageing time. Therefore, the drastic increase in RBP during second regime is attributed to the formation and growth of $Ni_3Ti$ and $Fe_2Mo$ intermetallic precipitates. It is also found that the increase in RBP during the second regime is 60% and where as the increase in hardness and microstrain are found to be 18% and 17%, respectively. Hence, RBP is more sensitive

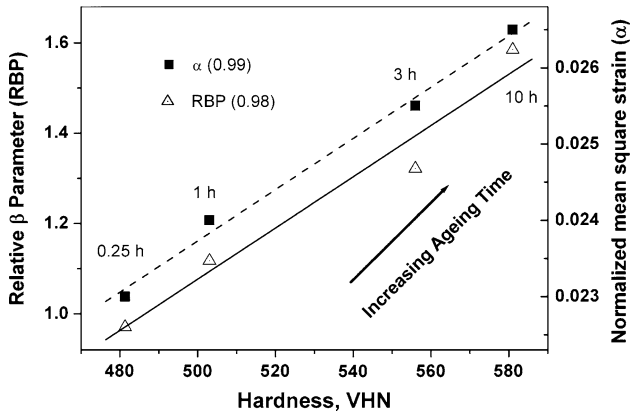


**Fig. 8** Variations of RBP and normalized mean square strain, α with respect to hardness during 0.25–10 h at 755 K

parameter during the second regime and can be used effectively for monitoring the changes due to ageing in this technologically important regime.

Upon prolonged ageing beyond 10 h, i.e. third regime, the RBP is found to decrease with ageing time. From Fig. 6, it is evident that the microstrain is also found to decrease for ageing durations above 10 h. Viswanathan et al. [6] and Guo et al. [10] have reported that precipitates will be coherent with matrix if their size is <11 nm, i.e. up to 10 h of ageing and beyond 10 h precipitates become incoherent with the matrix. Therefore, microstrain decreases for ageing duration greater than 10 h due precipitate coarsening. Hence, as explained earlier (Eq. 8), the RBP will also decrease at prolonged ageing durations due to coarsening of precipitates. During this regime, it is also found that the volume fraction of reverted austenite phase increases with ageing time, from 2, 5 to 30% as ageing time increases from 40, 70 to 100 h, respectively. At longer ageing durations above 40 h, the hardness is also found to decrease, which is attributed to the formation of soft reverted austenite. The BF image of the specimen aged at 755 K for 100 h is shown in Fig. 7c. It is observed that coarsening of $Ni_3(Ti,Mo)$ (marked as C) and globular $Fe_2Mo$ intermetallic precipitates (marked as D) and the presence of patchy continuous network of reverted austenite (marked as E) will take place at prolonged ageing of 100 h. These observations are different from the findings of Metya et al. [34] in C-250 grade maraging steel in which constant hardness after 12 h of ageing and drastic decrease in $\beta$ parameter were reported without any reference to the formation of reverted austenite.

Brezeale [40] reported that nonlinearity in solids is a function of crystalline structure. It is reported that nonlinearity is higher for metallic materials with BCC structure ($\beta \sim 5$ to 8.8) as compared to metallic materials with FCC structure ($\beta \sim 4$ to 7). Hence, it is expected that reversion of martensite (BCC) to soft austenite phase (FCC) will also be accompanied by a change in nonlinearity of the material. Hence, a plot is made between changes in volume fraction of reverted austenite and RBP, α and hardness as shown in Fig. 9. All these three parameters are seen to change with volume fraction of austenite in an identical manner. Thus, the decrease in RBP in the third regime, >10 h is attributed to the cumulative effect of precipitate coarsening and austenite reversion.

The studies reveal that NLU technique is sensitive to the microstructural changes that occur during ageing of M250 grade maraging steel and RBP can be used for identifying various substructural changes associated with precipitation hardening. However, systematic studies are necessary to understand the individual contributions of precipitate coarsening and austenite reversion on RBP. Nevertheless, the results presented here provide an illustration of how nonlinear ultrasonic technique can be useful for

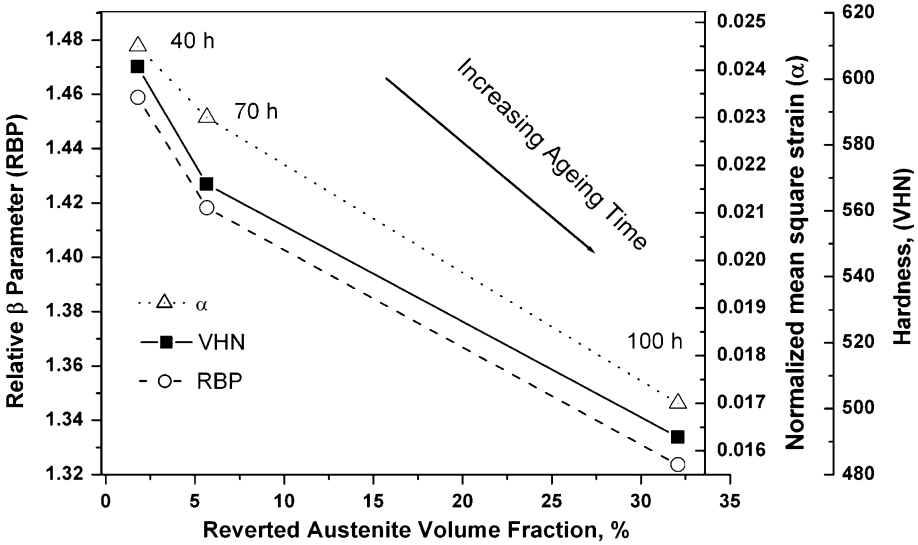


**Fig. 9** Variation of RBP, normalized mean square strain, α and hardness with volume fraction of reverted austenite

nondestructive characterization of microstructures in age hardened M250 grade maraging steel, especially, the three regimes of annihilation of dislocation during initial ageing, increase in coherency strains during intermediate ageing and formation of reverted austenite at prolonged ageing.

## Conclusion

From the nonlinear ultrasonic measurements carried out on M250 grade maraging steel specimens age hardened at 755 K for time durations in the range from 0.25 to 100 h, a systematic change in relative $\beta$ parameter (RBP) is observed with ageing time. The second harmonic amplitude is determined using pulse inversion technique for precise estimation of RBP. The first regime (SA–0.25 h) is characterized by marginal decrease (2.9%) in RBP up to 0.25 h of ageing due to the combined effect of two counteracting mechanisms operating simultaneously during the initial stages of ageing, i.e. dislocation annihilation and formation of very fine and coherent $Ni_3Ti$ precipitates. The second regime (0.25–10 h) is characterized by a drastic increase in RBP which is attributed to increase in microstrain due to precipitation and growth of coherent $Ni_3Ti$ and $Fe_2Mo$ intermetallic precipitates. The change in RBP is 60% for second regime. This is substantial compared to 18% increase in hardness and 17% increase in normalized mean square strain. Thus, RBP can be effectively used to study the ageing behaviour of technologically important second regime. At longer ageing durations beyond 10 h, i.e. in the third regime, RBP is found to decrease with ageing time due to the combined effect of coarsening of $Ni_3Ti$ and $Fe_2Mo$ precipitates and formation of soft reverted austenite. The present study clearly reveals that it is possible to use nonlinear ultrasonic $\beta$ parameter for characterization of microstructures in precipitation hardened M250 grade maraging steel.

**Acknowledgements** Authors thank Dr. K.V. Rajkumar, Scientific Officer, NDE Division, Indira Gandhi Centre for Atomic Research, Kalpakkam for many useful discussions.

## References

1. Weiss BZ (1982) In: Comins NR, Clark JB (eds) Specialty steels and hard materials. Pergamon press, Oxford, p 35
2. Vasudevan VK, Kim SJ, Wayaman CM (1990) Metall Trans A21:2655
3. Nakagawa H, Miyazaki T (2004) J Mater Sci 34:3901. doi:10.1023/A:1004626907367
4. Floreen S, Decker RF (1979) In: Decker RF (ed) Source book on maraging steels. ASM, Metals Park, OH, p 22
5. Decker RF, Floreen S, Wilson RK (eds) (1988) Maraging steels: recent developments and applications. TMS-AIME, Warrendale, PA, p 1
6. Viswanathan UK, Dey GK, Asundi MK (1990) Metall Trans A21:2429
7. Farooque M, Ayub H, Ul Haq A, Khan AQ (1998) J Mater Sci 33:2927. doi:10.1023/A:1004346412079
8. Sha W, Cerezo A, Smith GDW (1993) Metall Trans A24:1221
9. Sha W, Cerezo A, Smith GDW (1993) Metall Trans A24:1233
10. Guo Z, Sha W, Li D (2004) Mater Sci Eng A373:10
11. Habiby F, Siddiqui TN, Hussain H, Ul Haq A, Khan AQ (1996) J Mater Sci 31:305. doi:10.1007/BF01139144
12. Rajkumar KV, Anish Kumar, Jayakumar T, Baldev Raj, Ray KK (2007) Metall Trans A38:236
13. Rack HJ, Kailash RD (1971) Metall Trans A2:3011
14. Rajkumar KV, Rao BPC, Sasi B, Jayakumar T, Baldev Raj, Ray KK (2007) Mater Sci Eng A464:233
15. Habbiy F, Siddiqui TN, Khan SH, Ul Haq A, Khan AQ (1992) NDT&E Int 25:145
16. Pardal JM, Tavares SSM, Cindra Fonseca MP, da Silva MR, Neto JM, Abreu HFG (2007) J Mater Sci 42:2276. doi:10.1007/s10853-006-1317-8
17. Rajkumar KV, Vaidyanathan S, Anish Kumar, Jayakumar T, Baldev Raj, Ray KK (2007) J Magn Magn Mater 312:359
18. Mahadevan S, Jayakumar T, Rao BPC, Anish Kumar, Rajkumar KV, Baldev Raj (2008) Metall Trans A39:1978
19. Pardal JM, Tavares SSM, Cindra Fonseca MP, Abreu HFG, Silva JJM (2006) J Mater Sci 41:2301. doi:10.1007/s10853-006-7170-y
20. Rajkumar KV, Rajaraman R, Anish Kumar, Amarendra G, Jayakumar T, Sundar CS, Baldev Raj, Ray KK (2009) Philos Mag 89:1597
21. Hikata A, Chick BB, Elbaum C (1965) J Appl Phys 36:229
22. Hikata A, Elbaum C (1966) Phys Rev 144:469
23. Hurley DC, Blazar D, Purtscher PT, Hollman KW (1998) J Appl Phys 83:4584
24. Cantrell JH, Yost WT (2000) Appl Phys Lett 77:1952
25. Cantrell JH, Yost WT (1997) J Appl Phys 81:2957
26. Cantrell JH, Yost WT (1996) Rev Prog Quant Nondestruct Eval 15:1361
27. Hurley DC, Blazar D, Purtscher PT (2000) J Mater Res 15:2036
28. Hurley DC, Blazar D, Purtscher PT (2000) Mater Res Soc Symp Proc 591:129
29. Cantrell JH, Yost WT (2001) Int J Fatigue 23:S487
30. Frouin J, Stahish S, Matikas TE, Na JK (1999) J Mater Res 14:1295
31. Jhang K-Y, Kim K-C (1999) Ultrasonics 37:39
32. Jhang K-Y (2000) IEE Trans Ultrason Ferroelectr Freq Control 47:540
33. Pruell C, Kim J-Y, Qu J, Jacobs LJ (2007) Appl Phys Lett 91:231911
34. Metya A, Ghosh M, Parida N, Sagar SP (2008) NDT&E Int 41:484
35. Green RE Jr (1973) In: H Herman (ed) Treatise on material science and technology: ultrasonic investigation of mechanical properties Vol 3. Academic press New york, p 73
36. Kim J-Y, Jacobs LJ, Qu J (2006) J Acoust Soc Am 120:1266
37. Ohara Y, Kawashima K, Yamada R, Horio H (2004) Rev Prog Quant Nondestruct Eval 23:944
38. Muller T (2005) MSc Thesis, Georgia institute of technology, Atlanta, Georgia
39. Sinha PP, Sivakumar D, Babu NS, Tharian KT, Nataraj A (1995) Steel Res 66:490
40. Brezeale MA (1992) Rev Prog Quant Nondestruct Eval 11:2015